POLİTEKNİK DERGİSİ

JOURNAL of POLYTECHNIC

Size effect analysis of concrete beams under bending using crack-band approach

Eğilme altındaki beton kirişlerin çatlak-bant genişliği yaklaşımı ile boyut etkisinin analizi

***Yazar(lar) (Author(s))**: Bahar AYHAN[1], Erol LALE[2], Nilay ÇELİK[3]*

ORCID[1]: 0000-0001-9809-097X

ORCID[2]: 0000-0003-4895-5239

ORCID[3]: 0000-0002-7914-0086

Bu makaleye şu şekilde atıfta bulunabilirsiniz(To cite to this article): Ayhan B., Lale E. and Çelik N., "Size effect analysis of concrete beams under bending using crack-band approach", ***Politeknik Dergisi***, 25(2): 605-613, (2022).

Erişim linki (To link to this article): http://dergipark.org.tr/politeknik/archive

DOI: **10.2339/politeknik.762634**

Size Effect Analysis of Concrete Beams Under Bending Using Crack-Band Approach

Highlights

- *Three-point bending tests are simulated using Concrete damage plasticity model (CDPM) with FEM.*
- *CDPM is enhanced with crack band approach to prevent mesh dependency.*
- *Energy release rate is obtained by using J-integral approach.*
- *CDPM can capture experimental results as well as size effect law of Bazant.*
- *For future study, size effect analysis with CDPM under dynamic loading will be investigated.*

Graphical Abstract

Concrete damage-plasticity model (CDPM) enhanced with crack band approach is used to conduct size effect simulations of concrete specimens. The efficiency of this model is investigated.

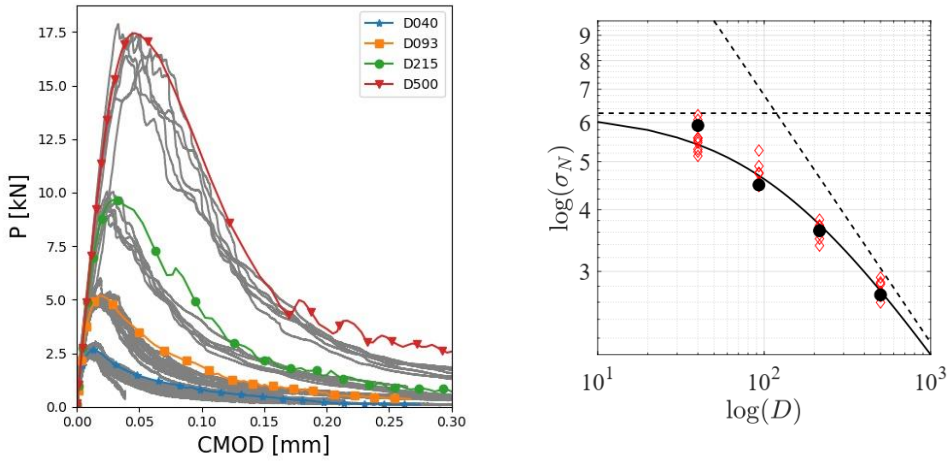

Figure. Comparison of obtained numerical results to experimental ones for $\alpha_o = 0.15$

Aim

The main aim of this study is to investigate the performance of the concrete damage plasticity model enhanced with crack band approach in capturing size effect.

Design & Methodology

Three-point bending tests are simulated to analyze size effect in notched and as well as in unnotched beams.

Originality

As far as authors knowledge, the size effect analysis of Hoover experiments using concrete damage plasticity model is not conducted before.

Findings

For the specimen for $L/D = 2.176$ *and which has a relative notch depth* $\alpha_o = 0.3$, *fracture energy and equivalent FPZ length are found as around 40 J/m*^{2} *and 17 mm, respectively.*

Conclusion

The concrete damage plasticity model enhanced with crack band approach can capture the size effect phenomenon very well.

Declaration of Ethical Standards

The author(s) of this article declare that the materials and methods used in this study do not require ethical committee permission and/or legal-special permissio

Size Effect Analysis of Concrete Beams Under Bending Using Crack-Band Approach

Research Article / Araştırma Makalesi

Bahar AYHAN[1, *], Erol LALE[1], Nilay ÇELİK[1]

[a]*Istanbul Technical University,Civil Engineering Department, Istanbul, 34469, Turkey*

(Received/Geliş 02.07.2020; Accepted/Kabul 22.11.2020 ; Erken Görünüm/Early View : 02.12.2020)

ABSTRACT

Analysis of size effect phenomenon in quasi-brittle materials is presented in this research using damage plasticity model. Notched and unnotched specimens under three-point bending fracture test are analyzed by setting a 3D finite element model. For this purpose, Abaqus software is utilized. Concrete damage-plasticity model (CDPM) enhanced with crack band approach is used to conduct simulations of concrete specimens. The efficiency of this model is investigated especially for size effect phenomenon. 2D finite element model is setup for three-point bending beams in order to estimate fracture parameters for specific span to depth ratio, L/D=2.176. The simulations are conducted for each different notch depths. 8-node quadratic plane stress elements are used to define 2D domain and singularity field at the notch tip is modeled using quarter point technique. Energy release rate is calculated using J-integral approach. Obtained results are compared to experimental ones reported in literature and are also compared to the Bazant's size effect law. This study shows that concrete damage-plasticity model enhanced with crack band approach can capture size effect observed in concrete-like materials' fracture.

Keywords: Size effect, crack band approach, mesh size independency, notch length, finite element analysis.

Eğilme Altındaki Beton Kirişlerin Çatlak-Bant Genişliği Yaklaşımı ile Boyut Etkisinin Analizi

ÖZ

Bu araştırmada, yarı gevrek malzemelerdeki boyut etkisinin hasar-plastisite modeli kullanılarak çözümlemesi sunulmuştur. Çentikli ve çentiksiz üç noktalı eğilme deneyleri üç boyutlu (3D) sonlu eleman modeli ile analiz edilmiştir. Bu amaçla, Abaqus yazılımı kullanılmıştır. Beton elemanların gerçekçi bir şekilde analizinde, özellikle boyut etkisinin dikkate alınmasında, çatlak bant genişliği yaklaşımı uygulanmış, hasar-plastisite modelinin etkinliği araştırılmıştır. Kırılma mekaniği parametrelerinin bulunması amacıyla, açıklık-yükseklik oranı, L/D=2.176, olan üç noktalı eğilme deneyine ait 2D sonlu eleman modeli, her bir çentik derinliği için oluşturulmuştur. Bu modelde, kiriş 8-düğüm noktalı dörtgen düzlem gerilme elemanları ile modellenmiş ve çatlak uç noktasındaki tekillik "quarter point" tekniği kullanılarak oluşturulmuştur. Bu analizler sonucunda, J-integral bulunmuş ve enerji salınım oranı hesaplanmıştır. Elde edilen sonuçlar literatürde verilmiş olan deney sonuçları ve ayrıca Bazant' ın boyut etkisi eğrisi ile karşılaştırılmıştır. Bu çalışma, çatlak bant genişliği yaklaşımı uygulanmış hasar-plastisite modelinin, beton gibi malzemelerde, boyut etkisini yakalamak için uygun olduğunu göstermiştir.

Anahtar Kelimeler: Çatlak analizi, ağ boyutu bağımsızlığı, çentik boyu, sonlu eleman modeli.

1. INTRODUCTION

Structural size effect phenomenon in quasi-brittle material such as concrete, wood, rock, stiff soils, ceramics etc., is a critical point to determine the strength resisted by the material. The region which contains a lot of distributed microcracks in front of the traction free crack tip is called as fracture process zone (FPZ) [1]. Internal structure of the material determines the size of FPZ.

The fracture behavior of a structure can be analyzed due to the size of this zone.

When compared to the dimension of the structure, if the FPZ size is insignificant, then linear elastic fracture mechanics (LEFM) governs the material behavior. On the other hand, if FPZ size is relatively big compared to the structural dimension, the behavior can be determined by a failure criterion of the plasticity. However, the zone size can have an intermediate size relative to size of structure, in this case the behavior is governed by a nonlinear fracture mechanics. Size effect can be investigated in a statistical (Weibull) way [2], [3] as well as in a deterministic (energetic) way [4], [5]. Bazant described two different types of size effect in quasi-brittle materials, especially for concrete. The first one is called "Type I" size effect, which is caused by the creation of finite size fracture process zone (FPZ), which involves the distributed microcracking and/or voids creation, without any existing crack. In this type of size effect, a macro-crack may initiate at many different points due to statistical distribution of weak locations in the structure. Second one, called "Type II" size effect, occur with a pre-defined crack, in other words failure location is known a priory.

**Corresponding Author*
e-mail: ayhanb@itu.edu.tr

Generally, standard continuum models are used to formulate the softening behavior in quasi-brittle materials. However, these models have a big handicap, which causes mathematically ill-posed problem in governing partial differential equations in case of softening, which manifest itself as mesh dependent result. For a remedy to this problem, Bazant and Oh [6] proposed crack band model. Main idea of the crack band approach is to adjust softening branch of the stress-strain curve according to finite element size, i.e. defining mesh-dependent softening curve, in order to provide same energy dissipation per unit area for different element sizes [6], [7], [8]. This adjustment can be done using fracture energy or displacement with crack bandwidth. It is widely used in several engineering simulations due to its simplicity.

On the other hand, mesh independent finite element simulations can be ensured by applying the non-local theory [9], [10]. Non-local models use a localization limiter, which is dependent on an internal structure of the material, that determine interaction zone. The integral type as well as gradient type nonlocal models are formulated in the literature. In integral type models, the stress is evaluated at each integration point by considering an internal (state) variable, which is determined as a weighted average of all integration points at the neighboring zone. In gradient type models, constitutive models depend on derivative of the equivalent strain. Hereby, mesh dependency, which are confronted in the local formulation, can be prevented. But these models are complicated and need more effort to define user-defined material models. They may cause excessive spread of damage which affects the performance of the models. In addition, discrete and particle models can be used to analyze quasi-brittle materials which have computationally high cost. Also, some advanced and rigorous high order continuum models are proposed based on discrete particle models [11] and successfully implemented to analyze quasi-brittle materials [12]. However, computational demands are also very high for this kind of models.

The primary objective of this research is to investigate the performance of the concrete damage plasticity model enhanced with crack band approach in capturing size effect. For this purpose, three-point bending simulations are performed to analyze size effect in notched and as well as in unnotched beams. The commercial finite element analysis software Abaqus [13] is utilized to set up finite element models.

2. MATERIAL MODEL

2.1 Damage Model

Concrete damaged plasticity model (CDPM) of Abaqus, which is capable of representing the behavior of quasi-brittle material, is used to characterize the tensile and compressive response of concrete. Isotropic damage and isotropic plasticity are used for the formulation of inelastic behavior. Tensile and compressive behavior of the model can be plotted for the uniaxial case as in Figure 1.

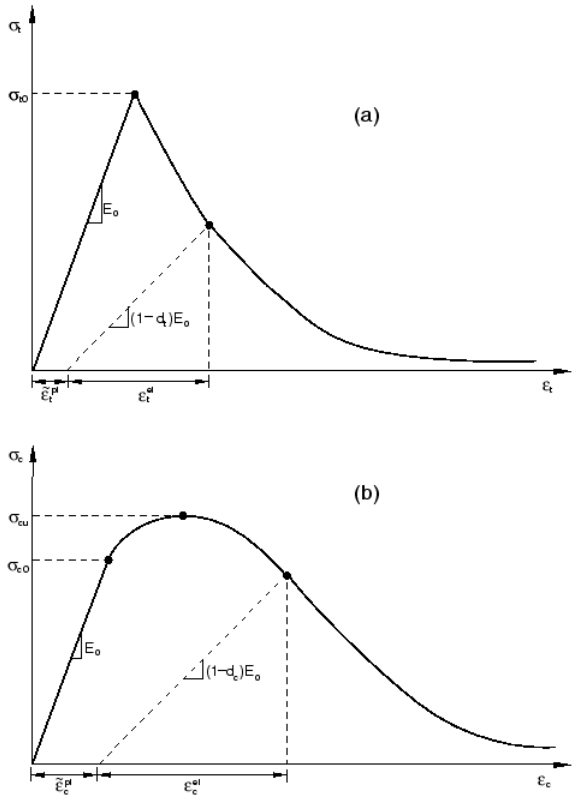

Figure 1. Response of concrete to uniaxial loading in tension (a) and compression (b), taken from [13]

Stress-strain relations under uniaxial tension and compression are expressed as below

$$\sigma_t = (1-d_t)E_o\left(\varepsilon_t - \tilde{\varepsilon}_t^{pl}\right)$$
$$\sigma_c = (1-d_c)E_o\left(\varepsilon_c - \tilde{\varepsilon}_c^{pl}\right) \quad (1)$$

where symbols *t* and *c* stand for tensile and compressive features. E_0 is the initial (undamaged) elastic stiffness of the material and $\tilde{\varepsilon}_{t,c}^{pl}$ refers to equivalent plastic strains for tensile and compressive strength, which control the evolution of yielding surface. This model uses two damage variables d_t and d_c to define the degradation of the elastic stiffness, which can take values from zero (undamaged state), to one (state for total loss of strength).

$$d_t = d_t\left(\tilde{\varepsilon}_t^{pl}\right); 0 \le d_t \le 1$$
$$d_c = d_c\left(\tilde{\varepsilon}_c^{pl}\right); 0 \le d_c \le 1 \quad (2)$$

For multiaxial loading, stress (σ) is obtained as

$$\sigma = (1-d)\bar{\sigma}$$
$$\bar{\sigma} = D_o^{el} : \left(\varepsilon - \varepsilon^{pl}\right) \quad (3)$$

Here, $\bar{\sigma}$ denotes effective stress and D_o^{el} is the initial (undamaged) elasticity matrix, *d* stands for damage in multiaxial loadings $d=(1-d_t)(1-d_c)$.

CDPM defines yield surface (F) and plastic flow potential (Φ) in effective stress space. Yield surface (*F*) [14, 15] , controlled by equivalent plastic strains, $\tilde{\varepsilon}_t^{pl}$ and $\tilde{\varepsilon}_c^{pl}$, considers different evolution of yield surface under tension and compression;

$$F=\frac{1}{1-\alpha}\left(\bar{q}-3\alpha\bar{p}+\beta\left(\tilde{\varepsilon}^{pl}\right)\left\langle\bar{\sigma}_{\max}\right\rangle-\gamma\left\langle-\bar{\sigma}_{\max}\right\rangle\right)-\bar{\sigma}_c\left(\tilde{\varepsilon}_c^{pl}\right)=0 \quad (4)$$

where $\bar{\sigma}_{\max}$ is the maximum principal effective stress. $\bar{p}$ and $\bar{q}$ denote first and second stress invariants, respectively. First invariant is the hydrostatic pressure $\bar{p}$ as;

$$\bar{p}=-\frac{1}{3}trace(\bar{\sigma}) \quad (5)$$

The second invariant is the von Mises equivalent effective stress $\bar{q}$ as

$$\bar{q}=\sqrt{\frac{3}{2}(\bar{s}:\bar{s})} \quad (6)$$

Here, $\bar{s}$ is the deviatoric part of the effective stress tensor, which can be shown as

$$\bar{s}=\bar{\sigma}+\bar{p}I \quad (7)$$

where *I* is the identity matrix. Moreover, in this yield function, some additional terms are defined as shown below:

$$\alpha=\frac{(\sigma_{b0}/\sigma_{c0})-1}{2(\sigma_{b0}/\sigma_{c0})-1};0\le\alpha\le0.5$$

$$\beta=\frac{\bar{\sigma}_c\left(\tilde{\varepsilon}_c^{pl}\right)}{\bar{\sigma}_t\left(\tilde{\varepsilon}_t^{pl}\right)}(1-\alpha)-(1+\alpha) \quad (8)$$

$$\gamma=\frac{3(1-K_c)}{2K_c-1}$$

Where σ_{bo},σ_{co} denote initial equibiaxial compressive yield stress and initial uniaxial compressive yield stress, respectively. K_C is the ratio of the second stress invariant on tensile meridian to compressive one, which determines the shape of the yield surface on deviatoric plane.

Non-associated plasticity approach is used by this model. Drucker-Prager hyperbolic function is used for plastic flow, which is described as follows,

$$\Phi=\sqrt{(\varsigma\sigma_{to}\tan\psi)^2+\bar{q}^2}-\bar{p}^2\tan\psi \quad (9)$$

Here ψ is the dilation angle measured in the hydrostatic versus deviatoric stress plane, $\sigma_{to}=\sigma_t\big|_{\tilde{\varepsilon}_t^{pl}=0,\dot{\tilde{\varepsilon}}_t^{pl}=0}$ is the uniaxial tensile stress at failure, ς is a parameter dealt with an eccentricity that defines the rate at which the function approaches the asymptotic line while $\varsigma\to0$. Default value of the eccentricity parameter is (0.1).

2.2 Tension Softening

Failure of concrete needs an appropriate description of strain softening because of the growing micro-cracks. For that reason, an expression or tabulated data needs to be given for the softening behavior of concrete. This softening curve can be linear, bilinear or exponential curve. It can be defined in terms of strain, which produces mesh dependent behavior. In order to prevent this, softening part should be defined in terms of fracture energy or displacement according to crack band theory.

3. SIZE EFFECT ANALYSIS

Once the peak loads for different sizes and geometries of specimens are obtained, a size effect formula, which is capable of comparing the results, is required. For this purpose, size effect law proposed by [16, 5] is performed in this study. Bazant developed size effect law based on effective crack length which is defined as the sum of a real stress-free crack "*a*" and a finite length of FPZ (c_f). The LEFM crack initiation condition is written as

$$G\left(\alpha_0+\frac{c_f}{D}\right)=\sigma_N^2\,D\,g\left(\alpha_0+\frac{c_f}{D}\right)/E' \quad (10)$$

Here, *G* denotes energy release rate. By expanding the term $g(\alpha_0+c_f/D)$ into Taylor series and taking only two terms, the nominal stress σ_N is obtained as

$$\sigma_N=\sqrt{\frac{E'G_f}{g'(\alpha_o)c_f+g(\alpha_o)D}} \quad (11)$$

In this expression, c_f is the effective length of fracture process zone that can be considered as a material parameter, *D* is the characteristic size of structure, $g(\alpha_o)$ is the dimensionless energy release function of equivalent linear elastic fracture mechanics dependent on the specimen geometry and α_o is relative initial crack length and $g'(\alpha_o)=\left.\frac{dg(\alpha)}{d\alpha}\right|_{\alpha=\alpha_o}$ is the first derivative of $g(\alpha_o)$, which can be estimated from the energy release rate as follows:

$$G(\alpha_o)=\frac{K_I^2}{E'}\sigma_N=\frac{\sigma_N^2D}{E'}g(\alpha_o) \quad (12)$$

Here, K_I is the stress intensity factor and $E' = E$ for plane stress, $E' = E/\left(1-\nu^2\right)$ for plane strain problems.

Values of $g\left(\alpha_o\right)$ and $g'\left(\alpha_o\right)$ can be taken from a handbook prepared for LEFM [17]. However, they are given for very limited geometries and loading conditions. For this reason, the energy release rate, $G\left(\alpha_o\right)$, is obtained numerically by using the software and the corresponding $g\left(\alpha_o\right)$ is calculated with the help of Eq.(12). G_f and c_f are the parameters which need to be identified according to experimental results. Identification procedure is explained in the next section. Once all these values are provided, size effect law diagram can be drawn.

4. NUMERICAL SIMULATIONS

Three-point bending tests done by [18] are selected to investigate performance of damage-plasticity model enhanced with crack band approach. The geometry of the concrete specimen is given in Figure 2. All dimensions of the beam are scaled with respect to depth, *D*. All beams have the same thickness, *b*, of 40mm. The initial notch width is taken as 2mm.

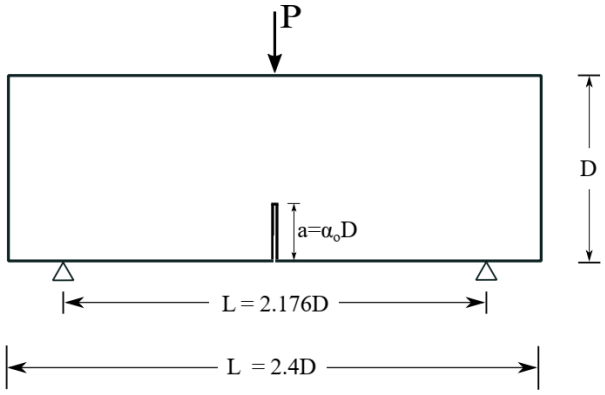

Figure 2. Notched beam under three-point bending

Hoover et al. tested four different size of the depth $D = \left[40, 93, 215, 500\right](mm)$ and all of them are considered for the analysis. It should be noted that the relative notch depth differs as $\alpha_o = \left[0.30, 0.15, 0.075, 0.025\right]$ for each depth size, *D*, of the beam.

Three dimensional (3D) finite element models are created in Abaqus. Quadratic (10-node) tetrahedral elements are used to model beam. Finer mesh size is used for the region close to the notch as seen in the Figure Figure 3. Beams are supported and loaded by using steel blocks, which are modeled with hexahedral finite elements assuming linear elastic material with modulus of elasticity $E = 200\,GPa$ and Poisson's ratio $\nu = 0.3.$ Dimensions of these plates are taken as reported in experimental study. Plates are tied to the beam via a penalty constraint algorithm. Center line of the plates is selected and boundary conditions are assigned on this line which enables rotation around it. For supporting plates, vertical and out of plane displacements are fixed and the other degrees of freedom (dof) are released. For the loading plate, displacement in longitudinal and out of plane direction is fixed. Beam is loaded in the vertical direction via prescribed velocity at the centerline of top plate.

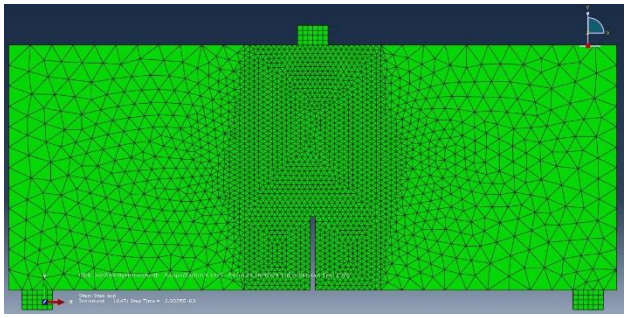

Figure 3. Mesh discretization of the specimen

4.1 Model Verification

For the preliminary study, the effect of mesh size is investigated to decide an optimum size for further analysis. The specimen with the dimension of $D = 215\left(mm\right)$ is considered. Moreover, a notch with a relative depth ratio $\alpha_o = 0.30$ is chosen among the others. The simulation is performed under a prescribed velocity on the top of the specimen. The elastic properties are taken as reported by [18] in which Young modulus is $E = 41240MPa$ and Poisson ratio is $\nu = 0.172$. The ratio of initial equibiaxial compressive yield stress to initial uniaxial compressive yield stress is assumed as $\sigma_{bo}/\sigma_{co} = 1.12$. Default value of K_C for the model considered is equal to 2/3.

The function proposed by Hordijk et al. [19, 20] is selected to define the tensile behavior of concrete, which is critical point of the problem. In that function, tensile yield strength changes from f_t value at undamaged condition to zero at the maximum width of the crack. Its expression is given as below:

$$\frac{f(u)}{f_t} = \begin{cases} \left(1+\left(c_1\frac{u}{u_{\max}}\right)^3\right)\exp\left(-c_2\frac{u}{u_{\max}}\right) - \frac{u}{u_{\max}}\left(1+c_1^3\right)\exp(-c_2) & if\ 0 < u < u_{\max} \\ 0 \quad if\ u_{\max} < u < \infty \end{cases} \tag{13}$$

where the constants c_1 and c_2 are 3 and 6.93, respectively. $f(u)$ is the stress due to the crack. u is the current crack opening and $u_{\max}$ is the maximum crack opening, which is calculated as

$$u_{\max} = 5.136\frac{G_f}{f_t} \tag{14}$$

Here, G_f is the fracture energy and f_t denotes the uniaxial tensile stress, which needs to be optimized.

The tensile strength and the fracture energy are selected as $f_t = 4MPa$ and $G_f = 30 Joule/m^2$ to fit the response of the chosen size with the experimental results.

Different mesh sizes are used in order to verify mesh independency of the model. For this purpose, central part of three-point bending specimen is discretized using tetrahedral elements with an edge size of 4, 2, 1 *mm* for coarse, medium and fine mesh, respectively.

Obtained numerical results are shown in the Figure 4. As can be seen, the results for medium and fine mesh are identical before peak and after peak there is a small discrepancy because of the dynamic nature of explicit solver. According to this result, medium size is selected for further simulations considering computational cost and time required for the analysis.

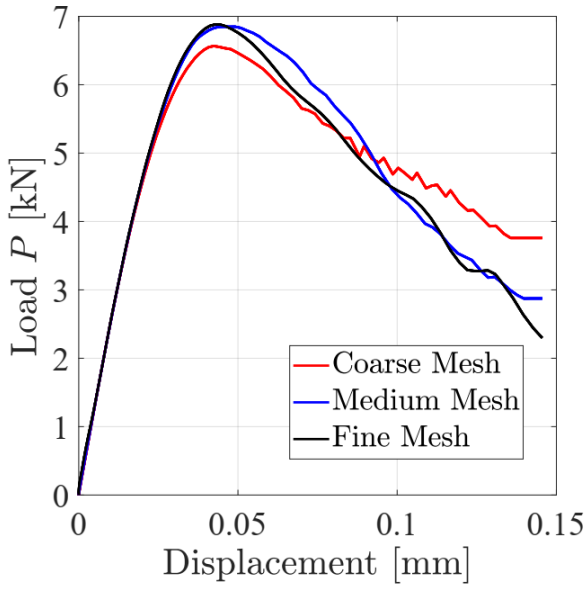

Figure 4. Load-displacement diagram for different mesh size

4.2 Numerical Results

In this section, load versus crack mouth opening displacement (CMOD) curves obtained from simulations are compared to experimental results with respect to different relative notch depths as shown in Figures Figure 5, Figure 6Figure 7Figure 8Figure 9. According to these figures, it is observed that numerical model can capture the experimental response for notched specimens, both in terms of strength and post-peak behavior. Additionally, for unnotched beams, obtained strength agrees with the experimental ones, as well. However, there is some discrepancy in post-peak part of curves. Authors believe that this is due to applied boundary conditions where friction forces are neglected between the supporting plates and the specimen.

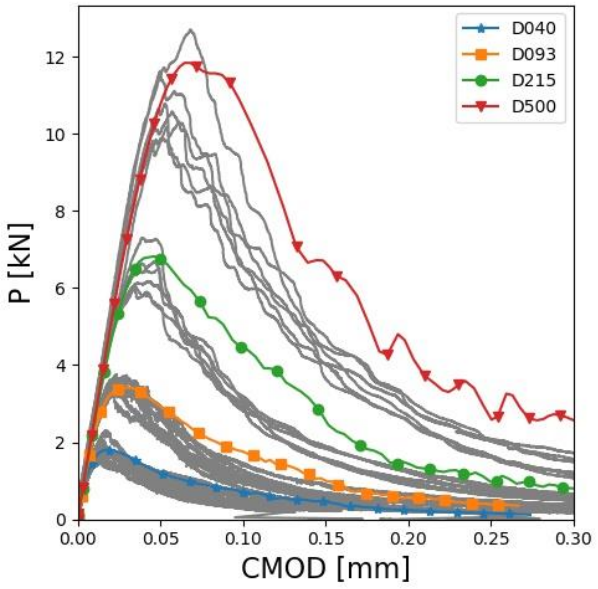

Figure 5. Comparison of size effect for the relative notch depth α_o=0.30. The gray curves represent the experimental results.

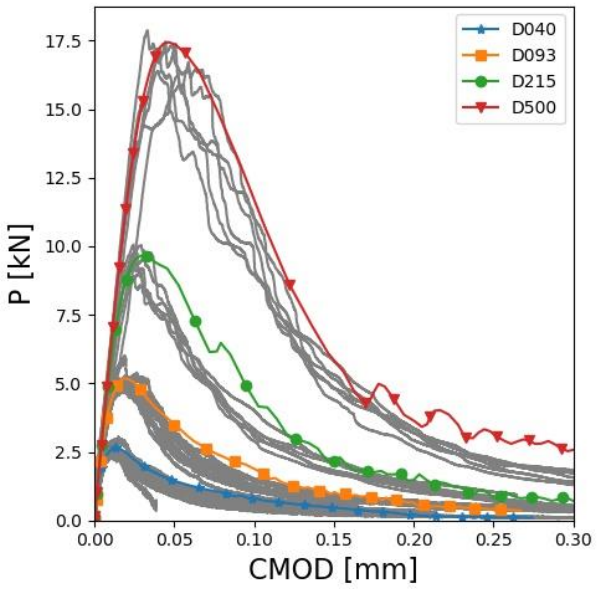

Figure 6. Comparison of size effect for the relative notch depth α_o=0.15. The gray curves represent the experimental results.

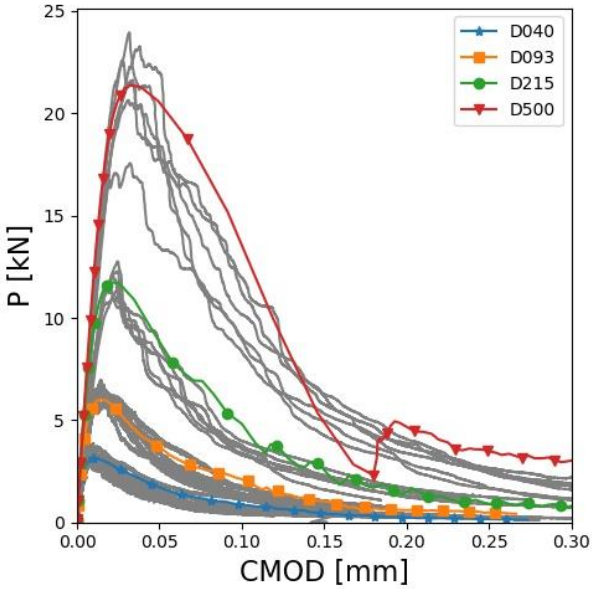

Figure 7. Comparison of size effect for the relative notch depth α_o=0.075. The gray curves represent the experimental results.

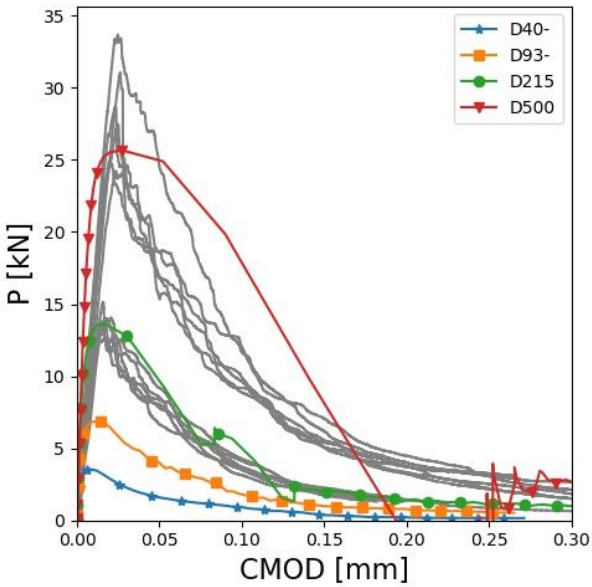

Figure 8. Comparison of size effect for the relative notch depth α_o=0.025. The gray curves represent the experimental results.

In Figure Figure 8, the curves of experiment for the depths of 40 and 93 mm cannot be plotted, because there is not any test done for these specimens.

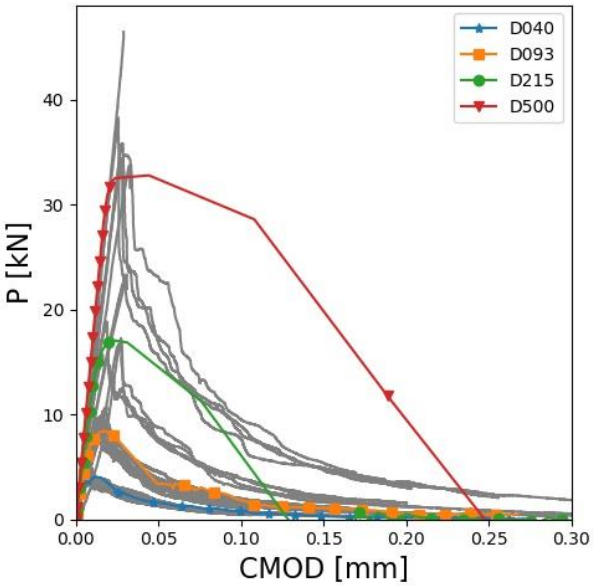

Figure 9. Comparison of size effect for the relative notch depth α_o=0. The gray curves represent the experimental results.

4.3 Behavior of Model for Size Effect

The influence of size effect for the crack band is examined according to the size effect law (SEL) [16].

Finite element model of three-point bending test are setup in order to estimate $g(\alpha_o)$ for specific span to depth ratio, $L/D = 2.176$, and relative notch depth, $\alpha_o = [0.3, 0.15, 0.075, 0.025]$. For this purpose, eight-node quadratic plane stress elements are used to define the domain. Moreover, singularity field at the notch tip is modeled using quarter point technique [13]. J-integral approach is used to get the energy release rate, $G(\alpha_o)$, which is employed to calculate $g(\alpha_o)$ by considering Eq.(12) for relative notch depths.

One needs to formulate g in terms of α to find $g'(\alpha_o)$. Thus, different values of α in the neighborhood of α_o are taken for computing the function of $g(\alpha)$. In this study, $\alpha = [\alpha_o - 0.02, \alpha_o - 0.01, \alpha_o, \alpha_o + 0.01, \alpha_o + 0.02]$ values are used and numerical results are interpolated with a fourth-degree polynomial and its derivative, $g'(\alpha_o)$, is obtained at α_o. Once these two values of $g(\alpha)$ and $g'(\alpha_o)$ are obtained, the energy fracture, G_f, and the effective length of FP, c_f, can be identified by using experimental results.

To determine these mentioned values above, Eq.(11) is rearranged to construct a linear function in the form of $y = ax + b$, as follows;

$$\frac{1}{\sigma_N^2} = \frac{g(\alpha_o)}{E'G_f} D + \frac{g'(\alpha_o)c_f}{E'G_f}$$
$$y = \frac{1}{\sigma_N^2}, \quad a = \frac{g(\alpha_o)}{E'G_f}, \quad b = \frac{g'(\alpha_o)c_f}{E'G_f} \tag{15}$$

where D is the variable of this function.

By having the experimental results from the work of Hoover et al [18]., we fitted an approximate curve through the points defining by the depth of the structure, D and the nominal stress, σ_N, expressed by the load applied, as shown below;

$$\sigma_N = \frac{3}{2}\frac{L}{D}\frac{P}{bD} \tag{16}$$

When the function of linear curve is determined, we obtained the coefficients a and b, which are used to calculate G_f and c_f ,respectively, by using Eq.(15). Identified parameters are summarized for each relative crack length in Table 1.

Table 1. Parameters for size effect law

α_o	$g(\alpha_o)$	$g'(\alpha_o)$	G_f	c_f
0.30	0.891097417	4.61994	4.011E-02	1.7796E+01
0.15	0.393335691	2.52075	4.421E-02	1.8429E+01
0.075	0.210765241	2.48064	4.467E-02	1.4074E+01
0.025	0.077631580	2.92275	-	-

By using these parameters, the results of the simulations and experimental ones are plotted against the Bazant's size effect curve in Figures Figure ***10***, Figure ***11*** and Figure ***12*** for different $\alpha_o = 0.3, 0.15, 0.075$ values, respectively. On the other hand, the diagram for $\alpha_o = 0.025$ is not plotted due to insufficient experimental results. In these figures, red diamond markers show experimental results, black circle ones show the simulation results and black solid curve indicates the size effect law. Also, the horizontal dashed line represents the plastic limit and inclined dashed line is LEFM limit, which has a slope of (0.5) in logarithmic scale.

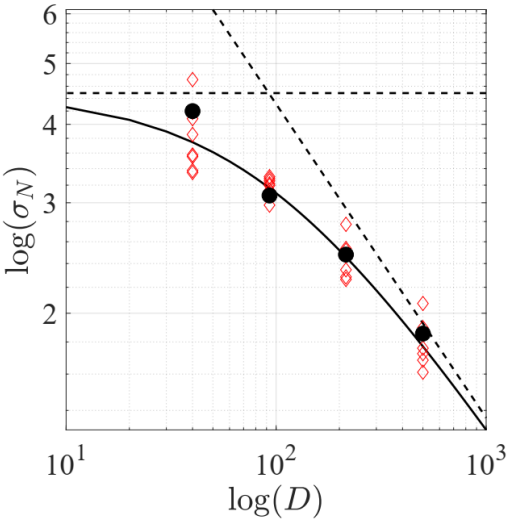

Figure 10. Size effect law for α_o=0.3

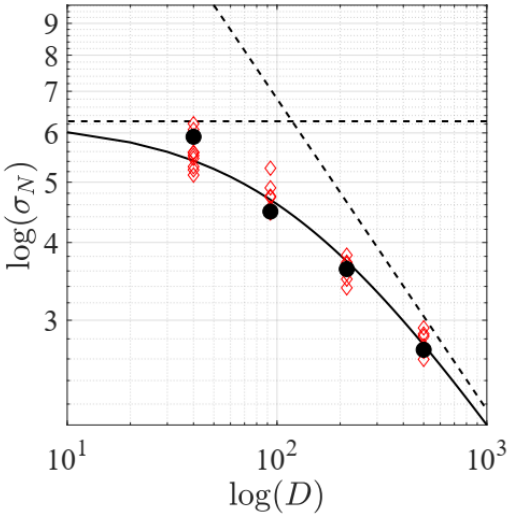

Figure 11. Size effect law for alpha=0.15

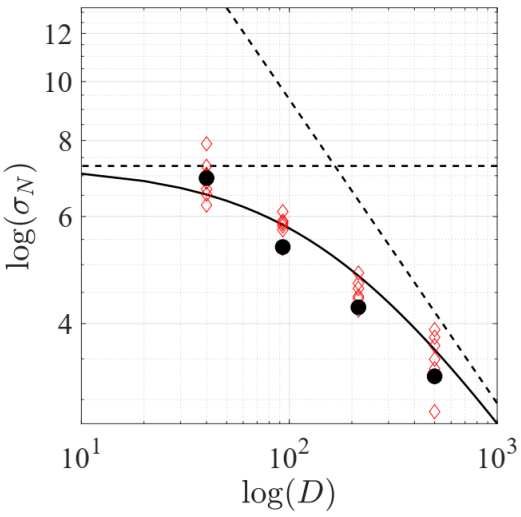

Figure 12. Size effect law for alpha=0.075

As can be seen from these figures, concrete damage plasticity model along with crack band approach can capture the size effect phenomenon quite well. Moreover, as expected, nominal strength is governed by LEFM for the higher structural size. Nevertheless, for small specimen size, nominal strength approaches asymptotically to the plastic limit.

5. CONCLUSION

This paper presents a size effect simulation by using CDPM enhanced with crack band approach. Three-dimensional finite element analysis is conducted using commercial software Abaqus. Crack mouth opening displacement (CMOD) versus load is drawn for beams, which have different notch depth. Obtained curves are compared to curves of three-point bending tests given by Hoover et al. Obtained results from simulation agree very well with the experimental ones.

Energy release rate for beam, which has span-to-depth ratio, L/D=2.176, is obtained by using J-integral taken from 2D finite element analysis. Once energy release rate is obtained, fracture characteristics are computed and given in this study. Size effect analysis of the numerical results are given and compared to experimental results as well as Bazant size effect law. It is shown that CDPM can capture size effect phenomenon quite well. As expected, strength is governed by LEFM for bigger specimen, on the other hand for small size specimen strength of the beam approaches to plastic limit.

For future study, size effect analysis with CDPM under high strain rate loading will be investigated.

DECLARATION OF ETHICAL STANDARDS

The author(s) of this article declare that the materials and methods used in this study do not require ethical committee permission and/or legal-special permission.

AUTHORS' CONTRIBUTIONS

Bahar AYHAN: Conceptualization of this study, Methodology, Software, Writing – review & editing original draft.

Erol LALE: Conceptualization of this study, Methodology, Software, Writing – review & editing original draft.

Nilay ÇELİK: Conceptualization of this study, Methodology, Software, Writing – review & editing original draft.

CONFLICT OF INTEREST

There is no conflict of interest in this study.

REFERENCES

[1] Hillerborg A., Modeer M. and Phtersson P.E., Analysis of Crack Formation and Crack Growth in Concrete by Means of Fracture Mechanics and Finite Elements, ***Cement and Concrete Research***, 6(6): 773-781, (1976).

[2] Bažant Z.P. and Pang S.D., Activation energy based extreme value statistics and size effect in brittle and quasibrittle fracture, ***Journal of the Mechanics and Physics of Solids***, 55(1): 91-131, (2007).

[3] Ballarini R., Pisano G. and Royer-Carfagni G., The Lower Bound for Glass Strength and Its Interpretation with Generalized Weibull Statistics for Structural Applications, ***Journal of Engineering Mechanics***, 142(12): (2016).

[4] Gonzalez K., Xue J., Chu A. and Kirane K., Fracture and Energetic Strength Scaling of Soft, Brittle, and Weakly Nonlinear Elastomers, ***Journal of Applied Mechanics***, 87:, (2020).

[5] Bažant Z.P. and Kazemi M.T., Determination of fracture energy, process zone length and brittleness number from size effect, with application to rock and concrete, ***International Journal of Fracture***, 44: 111-131, (1990).

[6] Bazant Z.P. and Oh B.H., Crack band theory for fracture of concrete, ***Matériaux et Constructions***, 16: 155-177, (1983).

[7] Jirásek M. ve Bauer M., Numerical aspects of the crack band approach, ***Computers and Structures***, 110-111: 60-78, (2012).

[8] Barbat G.B., Cervera M., Chiumenti M. and Espinoza E., Structural size effect: Experimental, theoretical and accurate computational assessment, ***Engineering Structures***, 213: , 110555, (2020).

[9] Havlásek P., Grassl P. and Jirásek M., Analysis of size effect on strength of quasi-brittle materials using integral-type nonlocal models, ***Engineering Fracture Mechanics***, 157: 72-85, (2016).

[10] Grégoire D., Rojas-Solano L.B. and Pijaudier-Cabot G., Failure and size effect for notched and unnotched concrete beams, ***Int. J. Numer. Anal. Meth. Geomech.***, 37: 1434-1452, (2013).

[11] Cusatis G. and Zhou X., High-order microplane theory for quasi-brittle materials with multiple characteristic lengths., ***Journal of Engineering Mechanics***, 140(7): 04014046, (2014).

[12] Lale E., Xinwei Z. and Cusatis G., Isogeometric Implementation of High-Order Microplane Model for the Simulation of High-Order Elasticity, Softening, and Localization, ***Journal of Applied Mechanics,*** 84(1): 011005, 2017.

[13] Simulia, ABAQUS User's Manual, Providence, RI: Dassault Systemes Simulia Corp., (2017).

[14] Lubliner J., Oliver J., Oller S. and Oñate E., A Plastic-Damage Model for Concrete, ***International Journal of Solids and Structures***, 25: 299-329, (1989).

[15] Lee J. and Fenves G.L., Plastic-Damage Model for Cyclic Loading of Concrete Structures, ***Journal of Engineering Mechanics***, 124(8): 892-900, (1998).

[16] Bažant Z.P. and Yu Q., Universal size effect law and effect of crack depth on quasi-brittle structure strength, ***Journal of engineering mechanics***, 135(2): 78-84, (2009).

[17] Tada H., Paris P.C. and Irwin G.R., The stress analysis of cracks handbook, New York: ASME Press, (2000).

[18] Hoover C.G., Bažant Z.P., Vorel J., Wendner R. and Hubler M.H., Comprehensive concrete fracture tests: description and results., ***Engineering fracture mechanics***, 114: 92-103, (2013).

[19] Cornelissen H., Hordijk D. and Reinhardt H., Experimental determination of crack softening characteristics of normalweight and lightweight, ***Heron***, 31(2): 45-46, (1986).

[20] Hordijk D. , Local Approach to Fatigue of Concrete, PhD Thesis: Delft University of Technology, (1991).